Identification and functional expression of a family of nicotinic acetylcholine receptor subunits in the central nervous system of the mollusc Lymnaea stagnalis

van Nierop, P.; Bertrand, S.; Munno, D.W.; Gouwenberg, Y.; van Minnen, J.; Spafford, J.D.; Syed, N.I.; Bertrand, D.; Smit, A.B.

published in
Journal of Biological Chemistry
2006

DOI (link to publisher)
10.1074/jbc.M508571200

document version
Publisher's PDF, also known as Version of record

THE JOURNAL OF BIOLOGICAL CHEMISTRY VOL. 281, NO. 3, pp. 1680–1691, January 20, 2006

Identification and Functional Expression of a Family of Nicotinic Acetylcholine Receptor Subunits in the Central Nervous System of the Mollusc *Lymnaea stagnalis*[*][S]

Received for publication, August 4, 2005, and in revised form, November 7, 2005 Published, JBC Papers in Press, November 11, 2005, DOI 10.1074/jbc.M508571200

Pim van Nierop[‡1], Sonia Bertrand[§], David W. Munno[¶], Yvonne Gouwenberg[‡], Jan van Minnen[‡], J. David Spafford[‖], Naweed I. Syed[¶], Daniel Bertrand[§], and August B. Smit[‡2]

From the [‡]Department of Molecular and Cellular Neurobiology, Center for Neurogenomics and Cognition Research, Faculty of Earth and Life Sciences, Vrije Universiteit, De Boelelaan 1087, 1081 HV Amsterdam, The Netherlands, the [§]Department of Neuroscience, University Medical Centre, 1, rue Midrel Servet, 1211 Geneva 4, Switzerland, the [¶]Department of Cell Biology and Anatomy, University of Calgary, T2N4N1 Calgary, Alberta, Canada, and [‖]Cellular and Molecular Neurobiology Research Group, University of Calgary, T2N 4N1 Calgary, Alberta, Canada

We described a family of nicotinic acetylcholine receptor (nAChR) subunits underlying cholinergic transmission in the central nervous system (CNS) of the mollusc *Lymnaea stagnalis*. By using degenerate PCR cloning, we identified 12 subunits that display a high sequence similarity to nAChR subunits, of which 10 are of the α-type, 1 is of the β-type, and 1 was not classified because of insufficient sequence information. Heterologous expression of identified subunits confirms their capacity to form functional receptors responding to acetylcholine. The α-type subunits can be divided into groups that appear to underlie cation-conducting (excitatory) and anion-conducting (inhibitory) channels involved in synaptic cholinergic transmission. The expression of the *Lymnaea* nAChR subunits, assessed by real time quantitative PCR and *in situ* hybridization, indicates that it is localized to neurons and widespread in the CNS, with the number and localization of expressing neurons differing considerably between subunit types. At least 10% of the CNS neurons showed detectable nAChR subunit expression. In addition, cholinergic neurons, as indicated by the expression of the vesicular ACh transporter, comprise ~10% of the neurons in all ganglia. Together, our data suggested a prominent role for fast cholinergic transmission in the *Lymnaea* CNS by using a number of neuronal nAChR subtypes comparable with vertebrate species but with a functional complexity that may be much higher.

Nicotinic acetylcholine receptors (nAChRs)[3] belong to the Cys loop family of pentameric ligand-gated ion channels (LGICs) together with the 5-HT_3, GABA type A/C, and glycine receptors. nAChRs consist of an extracellular ligand-binding domain (LBD), a transmembrane ion channel, and an intracellular domain (1). In the mammalian central nervous system (CNS), eight α-type (α2–7 and α9–10) and three β-type (β2–4). nAChR subunits have been identified that selectively assemble into nAChR subtypes with different pharmacology, cation conductance, and cellular localization. In the mammalian CNS, nAChRs predominantly mediate presynaptic modulation of neurotransmitter release (for example see Ref. 2) and are to a limited extent involved in direct, fast synaptic transmission (for example see Refs. 3–7). In contrast, in the molluscan CNS, the mode of fast synaptic cholinergic transmission seems to prevail. The CNS of the freshwater snail *Lymnaea stagnalis* consists of ~20,000 large and identifiable neurons, of which many were shown to express functional nicotinic acetylcholine receptors (8, 9). In particular, in well described neuronal networks, various nAChR subtypes were shown to mediate synaptic transmission (10, 11). Uniquely, molluscs possess excitatory and inhibitory nAChR subtypes conducting cations and anions, respectively (9, 12–15). Also, different excitatory and inhibitory nAChR subtypes mediate cholinergic transmission at single identified synapses, the differential contribution of which is regulated by soluble extracellular factors (11, 16). Therefore, functionally identified neurons in the *Lymnaea* CNS are a valuable model to explore nAChR function and diversity related to signal transmission in the nervous system. The lack of molecular information on nAChRs in molluscs, however, prevents a comprehensive analysis of cholinergic transmission. To address this issue, we identified nAChR subunits in the *Lymnaea* CNS, and we assessed their cellular expression by *in situ* hybridization and quantitative PCR. Our data underscore the postulated widespread role for fast cholinergic excitatory and inhibitory transmission in the *Lymnaea* CNS, involving a number of nAChR subtypes that are comparable with vertebrate species but with a functional complexity that may be much higher.

MATERIALS AND METHODS

Animals—Adult *L. stagnalis* (shell length, 28–34 mm) bred under laboratory standard conditions (17) were used.

PCR Using Degenerate Oligonucleotides—Total RNA was isolated using Trizol® reagent (Invitrogen) from freshly dissected CNS or from pooled LPeD1 (10×), RPeD1 (10×), and VD4 (6×) neurons with axons attached and isolated by mechanical suction from *Lymnaea* brain ganglia. For CNS preparations, mRNA was isolated using $(dT)_{26}$-coated magnetic beads (Dynal, Oslo, Norway). RNA was reverse-transcribed using hexanucleotide primers and Moloney murine leukemia virus-re-

* This work was supported in part by the Swiss National Science Foundation grant (to D. B.) and a Natural Science and Engineering Council of Canada grant (to N. I. S.). The costs of publication of this article were defrayed in part by the payment of page charges. This article must therefore be hereby marked "*advertisement*" in accordance with 18 U.S.C. Section 1734 solely to indicate this fact.

[S] The on-line version of this article (available at http://www.jbc.org) contains Fig. 5.

[1] Recipient of a grant from the Netherlands Organization for Scientific Research and Technology Foundation Stichting Toegepaste Wetenschappen (STW).

[2] To whom correspondence should be addressed: Dept. of Molecular and Cellular Neurobiology, Center for Neurogenomics and Cognitive Research, Faculty of Earth and Life Sciences, Vrije Universiteit, De Boelelaan 1085, 1081 HV Amsterdam, The Netherlands. Tel.: 31-20-5987116; Fax: 31-20-5987112; E-mail: guus.smit@falw.vu.nl.

[3] The abbreviations used are: nAChR, nicotinic acetylcholine receptor; CNS, central nervous system; LnAChR, *Lymnaea* nAChR subunit; LGIC, ligand-gated ion channel; GABA, γ-aminobutyric acid; LBD, ligand-binding domain; 5-HT, 5-hydroxytryptamine; nt, nucleotide; TM, transmembrane; CDC, caudodorsal cell; ACh, acetylcholine; AChBP, acetylcholine-binding protein; qPCR, quantitative PCR; LVAChT, *Lymnaea* vesicular ACh transporter; LYC, light yellow cells; LGC, light green cells; fwd, forward; rev, reverse; AL, anterior lobe; ISH, *in situ* hybridization.

verse transcriptase according to the manufacturer's protocol (Promega, Madison, WI).

3′- and 5′-directed degenerate oligonucleotides (Isogen Bioscience, Amsterdam, The Netherlands) were synthesized with an EcoRI or HindIII restriction site, respectively, at the 5′-ends. The 5′-directed oligonucleotides include the following: primer 1, 5′-cgggaattcaaytayaaymmiytigarmgnccngt-3′; primer 2, 5′-cggaattccarathhtigaygtigaygaraaraayca-3′; primer 5, 5′-cggaattcaarttyggiwsitggwsitaysrngg-3′; primer 7a, 5′-aagaattccngayrtistictitayaayaaygcnga-3′; primer 7b, 5′-aagaattccngayrtnstictitayaaywsigcnga-3′. The 3′-directed oligonucleotides include the following: primer 3, 5′-cgcaagcttswrttrtaiariariayrtcnggyttcca-3′; primer 4, 5′-cgcaagcttcantkytgiwcrtcraanggraacca-3′; primer 6, 5′-cgcaagcttayrtcirbrtaiggytcikkrcarca-3′; primer 8, 5′-tgtaagcttrtcrtaigwccaiswnccraaytt-3′ (nomenclature according to IUPAC).

Primer combinations were used on a CNS-derived cDNA (≥1 CNS equivalent) or on cDNA templates of identified neurons (0.12 cell equivalent for VD4 and 0.20 cell equivalent for LPeD1/RPeD1) in an initial PCR (40 cycles: 94 °C for 30 s; 54 °C for 30 s; and 72 °C for 90 s) using a DNA thermal cycler (PerkinElmer Life Sciences). Nested primers were used in a subsequent PCR (40 cycles: 94 °C for 30 s; 54 °C for 30 s; and 72 °C for 90 s) using 1/50th of the initial PCR as template. Amplified cDNA products were separated on 2% agarose gels, and generated products of expected sizes were excised, digested with EcoRI and HindIII, and cloned. For each independent PCR, several cloned products were sequenced by dideoxy chain termination sequencing.

Full-length Cloning—The cDNA of an amplified λZAPII (Stratagene, La Jolla, CA) cDNA library of the CNS of *L. stagnalis* was isolated by phenol extraction and ethanol precipitation. Nested oligonucleotide primer sets (Eurogentec, Seraing, Belgium) were designed based on partial PCR-derived nAChR subunit sequences. These primer sets were used together with nested λZAPII primer sets T33 (5′-gcgcaattaaccctcactaaagg-3′) and EV3 (5′-agcggataacaattttcacacagga-3′) or T77 (5′-gcgtaatacgactcactatagggcgc-3′) and EV2 (5′-cgccagggtttttcccagtcacgac-3′) in consecutive PCRs with identical parameters (40 cycles: 94 °C for 30 s; 58 °C for 30 s; and 72 °C for 210 s) using Advantage DNA polymerase (Clontech). DNA was separated on 1% agarose gels, and PCR products corresponding to 3′ (≥1000 bp) or 5′ (≥500 bp) parts were excised, cloned, and sequenced. Translation initiation sites were predicted using SMART (18). Final sequences were obtained by sequencing three independently generated PCR products generated on dT-primed cDNA of pooled *Lymnaea* CNS. For *Xenopus* oocyte expression, cDNAs of open reading frames were cloned into pcDNA3 (Invitrogen). Sequences of cloned products were checked by dideoxy chain termination sequencing.

Sequences of cloned products were checked by dideoxy chain termination sequencing. GenBank™ data base accession numbers for the sequences are as follows: LnAChR A, DQ167344; LnAChR B, DQ167345; LnAChR C, DQ167346; LnAChR D, DQ167347; LnAChR E, DQ167348; LnAChR F, DQ167349; LnAChR G, DQ167350; LnAChR H, DQ167351; LnAChR I, DQ167352; LnAChR J, DQ167354; LnAChR K, DQ167353; and LnAChR L, DQ167355.

Sequence Analysis—Protein alignments were performed with ClustalX (19). Secondary structure elements of deduced protein sequences were predicted using SMART (18). Biologically active sites were predicted from the Prosite data base using ScanProsite (20, 21). Probability of phosphorylation sites was analyzed by using NetPhos 2.0 (22). Phylogenetic analysis was performed by ClustalX using the neighbor-joining method (Kimura correction). Regions of weak alignment (corresponding to residues 13–15, 166–167, 298–434, and 460–462 of LnAChR A) were excluded from the analysis.

TABLE 1

Cloning strategy of Lymnaea nAChR subunits

A, *Lymnaea* nAChR subunits were identified by PCR using degenerate oligonucleotides in two consecutive rounds of amplification on various cDNA templates. Products generated by these reactions correspond to three regions of the LGIC LBD, referred to as regions A, B, and C (see also Fig. 1), and were named accordingly. Partial products A3 and C4, C1 and B2, and B1 and C3 represented partial sequences of single RNA transcripts. B, partial LnAChR sequences X1 and X2 were obtained from a phage-library screen[4] and an EST sequencing project (L. L. Moroz, University of Florida).

A

primers 1st amplification	primers 2nd amplification	cDNA templates	generated product	LnAChR subunit
primer 1 primer 4	primer 2 primer 4	total CNS	A1	LnAChR A
			A2	LnAChR L
			A3	LnAChR B
			A4	LnAChR C
			A5	LnAChR D
		RPeD1	-	-
		LPeD1	-	-
		VD4	-	-
primer 7a/b primer 8	primer 7a/b primer 8	total CNS	B1	LnAChR G
		RPeD1	B2	LnAChR E
			B3	LnAChR I
		LPeD1	B1	LnAChR G
		VD4	-	-
primer 5 primer 6	primer 5 primer 6	total CNS	C1	LnAChR E
			C2	LnAChR F
			C3	LnAChR G
			C4	LnAChR B
			C5	LnAChR H
		RPeD1	-	-
		LPeD1	-	-
		VD4	C2	LnAChR F

B

source			
λ-phage-library screen	total CNS	X1	LnAChR J
EST-sequencing project	total CNS	X2	LnAChR K

Electrophysiology—*Xenopus laevis* oocytes were prepared, injected, and recorded as described previously (23). Drugs were applied in the bath by rapid superfusion that was controlled by electromagnetic valves. Drugs and chemicals were purchased either from Sigma or Fluka. Current-voltage relationships (I-V curves) were determined either by holding the cell at a fixed potential and measuring the ACh-evoked current or by voltage ramps (from −100 to + 80 mV in 2 s) applied during the ACh response. I-V plots were obtained by reporting the amplitude of the current as a function of the holding voltage after subtraction of the passive cell properties determined in absence of the agonist.

Real Time Quantitative PCR—RNA of the complete CNS, individual ganglia, and body tissues was isolated as described above followed by a DNase I (10 units; Roche Applied Science) treatment, according to the manufacturer's instructions, and by phenol/chloroform extraction and ethanol precipitation. cDNA was made using hexanucleotides (300 pmol) and 200 units of Moloney murine leukemia virus H-reverse transcriptase (Promega, Madison, WI). RNA from pooled VD4 (6×) and LPeD1 (6×) neurons, cultured for 18 h, was isolated, and hexanucleotide-primed cDNA was transcribed according to van Minnen and van Kesteren (24).

All cDNAs were ethanol-precipitated and dissolved in 60 μl of aquadest. Transcript-specific primers were designed using Primer Express (Applied Biosystems, Foster City, CA) to generate 70–120-bp amplicons as follows: LnAChR A fwd, 5′-gctaggaatgacctggaatgc-3′, and LnAChR A rev, 5′-ggaacccacaccatctgctta-3′; LnAChR B fwd, 5′-tccagtttcgctacccagatg-3′, and LnAChR B rev, 5′-gcgttggactcgacgatgt-3′; LnAChR C fwd, 5′-tgactcaacgtggtgtgcaa-3′, and LnAChR C rev, 5′-aacccaatgattccatgga-3′; LnAChR D fwd, 5′-cagaatggaccgaccagaaa-3′, and

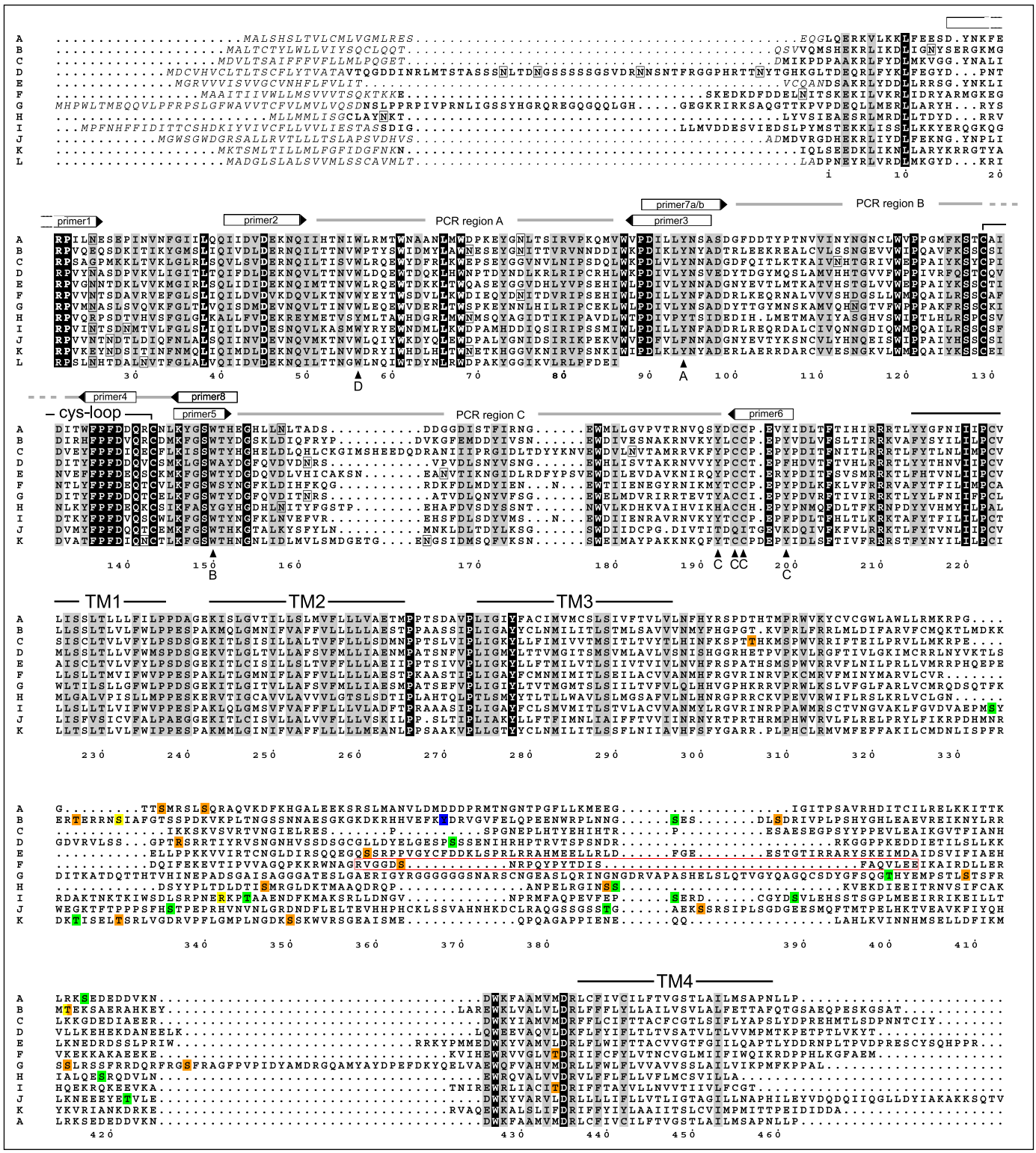

FIGURE 1. **Deduced protein sequences of LnAChR subunits.** ClustalX alignment of deduced protein sequences of identified LnAChR A–L subunits. Residue numbering *below* the alignment is set to the mature LnAChR A sequence. Positions and names of primers used for amplification are indicated, as well as three regions of amplification delineated by the applied primer combinations (*gray lines*). Positions of identical and conserved amino acids are indicated (*black* and *gray columns*, respectively). The alignment shows putative signal peptides (*italic*) and transmembrane domains (labeled *TM1, TM2, TM3*, and *TM4*) as predicted by SMART analysis (18). Indicated are the conserved Cys pair that defines the Cys loop family of LGIC subunits, the conserved residues of the principal (*loops A–C*), and the complementary component (*loop D*) of the ligand-binding site (*arrowheads*). Also represented are sites in the LBDs of possible *N*-linked glycosylation (*black boxes*) and of predicted sites in the long intracellular loop of phosphorylation by cAMP and cGMP-dependent kinases (*yellow shading*), casein-dependent kinase (*green shading*), protein kinase C (*orange shading*), and tyrosine kinases (*blue shading*). Only phosphorylation sites as predicted by Prosite analysis with a significant score in NetPhos are represented. The alternatively spliced region in the long intracellular loop of LnAChR F is indicated (*red box*).

LnAChR D rev, 5′-cgacaaggtattctgagccgttt-3′; LnAChR E fwd, 5′-cgcggtcaagaacattcga-3′, and LnAChR E rev, 5′-acggtgtggaacagggtcttt-3′; LnAChR F fwd, 5′-atcctggatgtggacgtcaaa-3′, and LnAChR F rev, 5′-cacgtccgaccaagtatattcgt-3′; LnAChR G fwd, 5′-ggctttcaggtggacataacg-3′, and LnAChR G rev, 5′-tcaccgctgaacacgtagttc-3′; LnAChR H fwd, 5′-tctcaggctgtctggcgtaca-3′, and LnAChR H rev, 5′-cagatcccgcatcagtcttga-3′; LnAChR I fwd, 5′-agtggatgccccaagctattc-3′, and LnAChR I rev, 5′-ggtccacgagccaaacttaagc-3′; LnAChR J fwd, 5′-gctgaacgctcctcacattct-3′, and LnAChR J rev, 5′-tcgagcaacccttggatga-3′; LnAChR K fwd, 5′-ccctttcgacatccaaaattg-3′, and LnAChR K rev, 5′-accgtccatgctcagtaccat-3′; LnAChR L fwd, 5′-ttgacaacaaacggttggttaaat-3′, and LnAChR L rev, 5′-aatggcaacctcaggaccttt-3′; LEFa fwd, 5′-accacaactggccacttgatc-3′, and LEFa rev, 5′-ccatctcttgggcctctttct-3′; Ltub fwd, 5′-caagcgcatctctgagcagtt-3′, and Ltub rev, 5′-tggattccgcctctgtgaa-3′; and LVAChT fwd, 5′-cgaactgtgagattggtttgatg-3′, and LVAChT rev, 5′-tcaccctctgttgtttccataactt-3′.

Quality testing of primers and qPCRs were performed as described earlier (25). C_t values were used to calculate the relative expression level ($C_{t,\mathrm{norm}}$) normalized to *Lymnaea* β-tubulin (Ltub; GenBank™ accession number X15542) or *Lymnaea* elongation factor α (LEFα; GenBank™ accession number DQ278441). For gene x, the $C_{t,\mathrm{normgenex}}$ is calculated as follows: $C_{t,\mathrm{genex}} - C_{t,\mathrm{Ltub}}$. These values were transformed to yield linear expression levels for each sample by $Pe\text{-}C_{t,\mathrm{normgenex}}$, where P is the amplification efficiency of the primer set. For each set, the amplification efficiency was determined once on serial template dilutions. Normalized linear gene expression levels from replicate measurements were expressed as the mean ± S.E. On preparations of CNS, ganglia, and neuronal population, expression of all transcripts was detected with the highest C_t value (lowest abundance) measured at least six cycles (factor 32) below the no-template control.

In Situ Hybridization—In situ hybridization was performed as described previously (26). Specific [^{32}P]UTP-labeled RNA probes were transcribed from linearized cDNA (200 ng) corresponding to stretches of coding sequence of LnAChR A (nts 1039–1380), B (nts 1096–1470), C (nts 1035–1395), D (nts 1011–1556), E (nts 895–1472), F (nts 986–1357), G (nts 1341–1767), H (nts 909–1293), I (nts 1209–1523), J (nts 894–1503), K (nts 959–1386), L (nucleotides gtccgccaagaattttggc in 5′-untranslated region-365), and LVAChT (nts 1–407; GenBank™ accession number AF484093). *In situ* hybridization (ISH) probes for nAChR subunits were designed to minimize cross-hybridization and, where possible, target regions that encode the intracellular TM3–TM4-connecting loop that has a very low degree of sequence conservation.

RESULTS

Identification of nAChR Subunits from the CNS of L. stagnalis—For the identification of nAChR subunits, we performed a nested PCR using degenerate primers on various CNS-derived cDNA templates (Table 1A). Sequencing of amplified DNA identified 13 different sequences that each showed similarity to a region of the LBD of nAChR subunits (see also Fig. 1). In addition, two sequences representing partial *Lymnaea* nAChR subunits were available from previous hybridization screening of a λ phage CNS cDNA library for nAChR subunit-related sequences[4] and from an ongoing *Lymnaea* CNS EST sequencing project (L. L. Moroz, University of Florida) (Table 1B). Full-length sequence information of the partial sequences was obtained by PCR cloning using a *Lymnaea* CNS cDNA library. In total, 12 individual transcripts were identified that were named *Lymnaea* nAChR subunits (LnAChR) A–L (Fig. 1). A full-length sequence for LnAChR L could not be obtained. For LnAChR F, a splice variant was identified yielding sequence diversity in the long intracellular loop between TM3 and TM4. The alternatively spliced region in LnAChR F contains a predicted protein kinase C phosphorylation site (NetPhos score 0.948) (Fig. 1).

With BLAST analysis each of the 12 deduced protein sequences share highest similarity with predicted as well as with functionally characterized nAChR subunits (data not shown). Sequence comparison with human LGIC subunits indicates the highest identity with nAChR subunits (Fig. 2*C*). Previously described *Lymnaea* GABA receptor subunits (27, 28) do not show significant sequence identity with the identified protein sequences. All identified proteins possess four predicted transmembrane domains (TMs) with a relative spacing (three TMs at the center and one TM at the C terminus) that are similar to the organization observed in nAChR subunits. Moreover, the subunits contain two cysteine residues separated by 13 amino acids (Fig. 1), which are features characteristic for proteins belonging to the so-named Cys loop family of LGICs.

Together, these results support the classification of the identified sequences as *Lymnaea* nAChR subunits. Because of the presence of the typical vicinal Cys residues in the loop C region of the principal component of ligand binding, LnAChR A–I and LnAChR K are classified as α-type nAChR subunits, and because of the absence of these Cys residues, LnAChR J is classified as β-type subunit. Most interestingly, in loop C the LnAChR H subunit shows an unusual His-*X*-Cys-Cys-*X*-*X*-*X*-Tyr motif rather than the conserved Tyr-*X*-Cys-Cys-*X*-*X*-*X*-Tyr.

Sequence Comparison of Lymnaea nAChR Subunits—Of all identified subunits, LnAChR F and I share the highest level of sequence identity (69% identity), whereas LnAChR H and K share the lowest level (25% identity) (Table 2A). For comparison, human nAChR subunits share sequence identity values of 35–84% (data not shown). LnAChR E shares the highest sequence identity with the α2 and α4 nAChR subunits (62%), whereas the lowest identity is found for LnAChR H and the human β2 subunit with only 24% identical residues (Table 2B).

Based on sequence relatedness (Table 2A), we defined three group of LnAChR subunits each with >60% inter-sequence identity, group B, I, and F, group C and E, and group D and G (Fig. 2*A*). None of the LnAChR subunits LBD domains displays a particular homology to AChBP, a molluscan protein secreted by glial cells homologous to the nAChR LBD (29, 30) (Fig. 2*B*). AChBP shares the highest sequence identity (27%) with the LnAChR K subunit (see Table 2A). The groups of subunits that include LnAChR H, the LnAChR B, F, I, and K, and the LnAChR D and G subunits branch off between human 5-HT$_3$ receptors and nAChR subunits (Fig. 2*C*). Based on phylogeny, LnAChR H seems as distant from 5-HT$_3$ subunits as it is from nAChR subunits. Most interestingly, LnAChR A displays a clear relation to the vertebrate α7 subunit that forms homopentameric receptors, whereas LnAChR J, C, and E are more related to subunits known to assemble into heteropentameric nAChRs.

Functional Expression of LnAChRs in Xenopus Oocytes—To determine the contribution of LnAChR subunits to functional receptors, we expressed LnAChR subunits in *X. laevis* oocytes. As a first step, LnAChR subunits were expressed individually allowing for only homopentameric nAChR subtypes to be formed. Expression of functional receptors was observed with LnAChR A or B subunits and with LnAChR I subunits (Fig. 3*A*). Oocytes that express the LnAChR A or B subunits responded to application of ACh but not to application of 5-HT (Fig. 3, *B* and *C*), glutamate, GABA, or glycine (data not shown). Receptors composed of LnAChR A or B subunits are sensitive to typical nicotinic agonists (*i.e.* nicotine and choline) and antagonists (*i.e.* meth-

[4] E. Vreugdenhil and A. B. Smit, unpublished data.

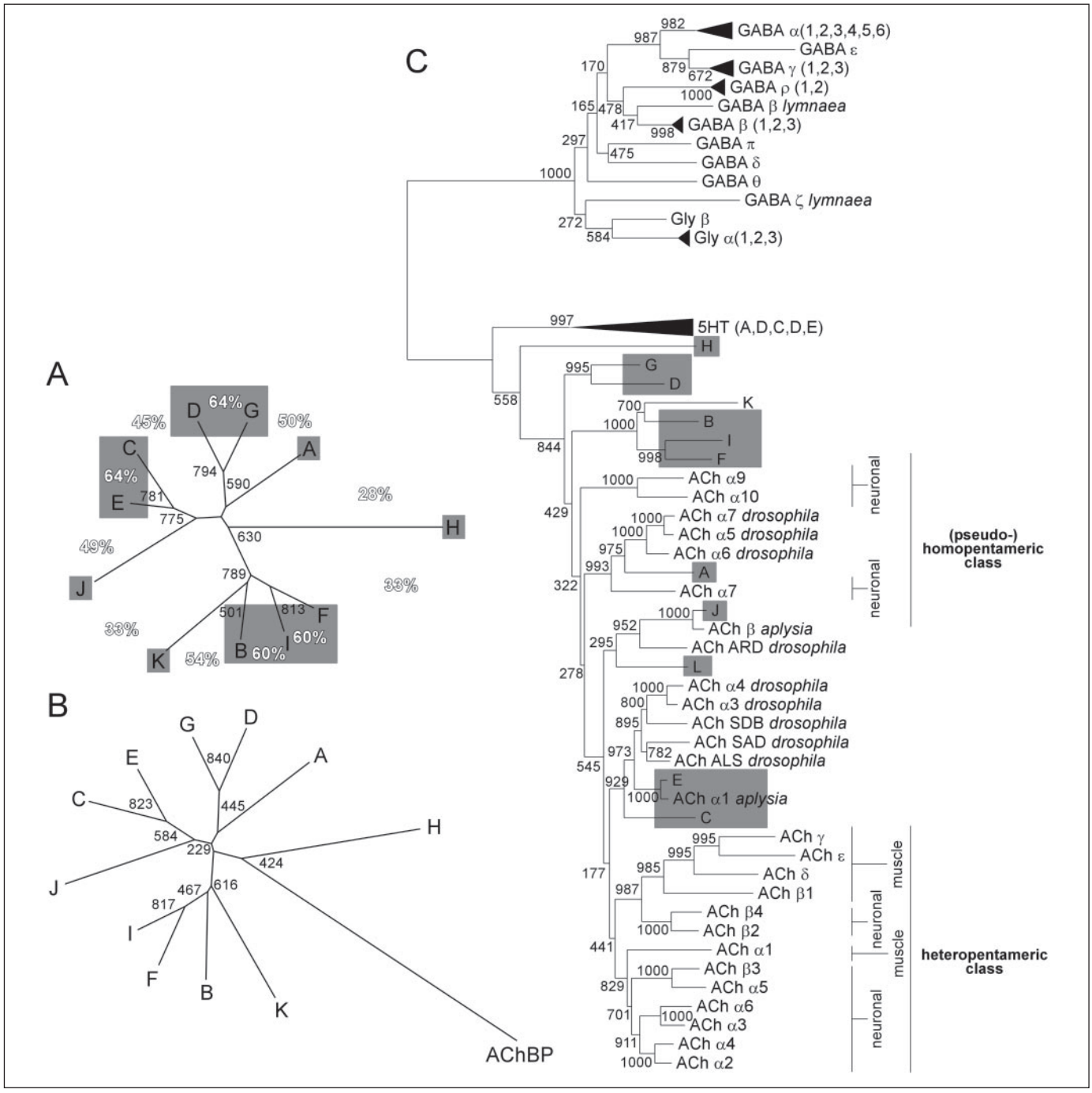

FIGURE 2. **Phylogenetic comparison of LnAChR subunits.** *A,* phylogenetic tree of LnAChR subunits. Values of bootstrap analysis on 1000 data sets are indicated at branch points (*black numbers*). Sequence identity values are indicated for adjacent proteins (*outlined numbers*). Groups of LnAChR subunits with a ≥60% identity score (see Table 2) are highlighted (*gray boxes*). The partial LnAChR L sequence shows no particular relationship to any other subunit (data not shown). *B,* the procedure as under *A* was repeated, including AChBP now aligning residues belonging to regions corresponding to AChBP and the corresponding LBD of LnAChR subunits. The partially identified LnAChR L subunit was not included. *C,* phylogenetic tree of LnAChR subunits and all subunits that belong to the Cys loop family of LGICs identified in *Aplysia*, *Lymnaea*, *Drosophila,* and human. Values of bootstrap analysis on 1000 data sets are indicated at branch points. Related LnAChR subunits as defined under *A* are indicated (*gray boxes*). For human nAChR subunits, participation in the formation of neuronal or muscle nAChRs and of homo- or heteropentameric nAChRs are indicated. *Black triangles* indicate compressed sub-trees of closely related subunit types. Names indicate human subunits unless stated differently. Subunit sequences were received from the LGICdb (56).

yllycaconitine, dihydro-β-erythroidine, α-bungarotoxin, and α-conotoxin-ImI) (57). Although recorded currents are smaller, oocytes expressing the LnAChR I subunit respond equally to ACh or 5-HT applications (Fig. 3*D*). LnAChR I receptors are also insensitive to glutamate, GABA, and glycine (data not shown).

The failure of many subunits to express as functional receptors as well as the small size of the currents mediated by receptors composed of the LnAChR I subunit suggests that additional subunits are required for functional expression. As a second step, subunit combinations were selected based on the inferred subunit classification and similarity of expression levels in the CNS (see Fig. 5). Co-expression of the β-type LnAChR J subunit with other subunits, including those resembling most the α-subunits found in mammalian neuronal nAChRs (LnAChR C or E), did not result in functional channels. Moreover, no currents

TABLE 2

Protein sequence identity of Lymnaea and rat nAChR subunits

A, distance matrix of sequence identity (%) of aligned LnAChR subunits and *Lymnaea* AChBP (GenBank™ accession number P58154). B, distance matrix of identity scores (%) of aligned LnAChR and human nAChR subunits. The long intracellular loop was excluded from comparison. Dark and light boxes indicate the highest and lowest scores for each LnAChR subunit, respectively.

A

	A	B	C	D	E	F	G	H	I	J	K	L*	AChBP*
A		42	45	48	47	41	50	28	41	41	38	49	23
B			42	41	45	59	42	32	59	38	54	39	24
C				45	64	40	47	30	42	46	37	41	24
D					48	42	64	33	43	35	34	47	23
E						42	50	29	40	49	38	50	23
F							46	33	69	39	47	43	25
G								34	43	42	38	43	23
H									33	27	25	30	23
I										39	48	40	23
J											33	47	20
K												26	27
L*													14
AChBP*													

B

	ACHa1hosa	ACHa2hosa	ACHa3hosa	ACHa4hosa	ACHa5hosa	ACHa6hosa	ACHa7hosa	ACHa9hosa	ACHa10hosa	ACHb1hosa	ACHb2hosa	ACHb3hosa	ACHb4hosa	ACHdhosa	ACHehosa	ACHghosa
A	43	46	44	46	40	46	54	43	43	38	42	41	41	37	31	36
B	35	42	40	41	42	37	41	38	39	32	38	38	37	32	30	32
C	47	53	52	53	46	50	47	44	46	40	50	50	48	42	35	39
D	40	43	40	41	39	39	44	42	42	35	37	35	40	34	34	36
E	52	62	58	62	55	56	49	47	44	45	59	57	58	43	39	40
F	35	41	37	41	35	35	38	39	37	33	35	32	36	32	31	32
G	43	47	43	46	43	43	46	43	46	39	43	43	43	39	34	36
H	31	31	33	33	31	32	31	29	29	31	26	30	31	26	28	29
I	33	40	35	39	34	35	37	39	39	30	34	35	35	29	28	29
J	44	51	50	52	46	47	41	39	40	41	50	47	45	41	36	39
K	33	36	33	36	36	32	36	38	36	28	33	33	35	28	29	28
L*	49	51	43	50	49	49	45	40	44	39	43	50	40	38	32	43

* Data analyzed on partial sequence.

could be observed with subunits combinations, including both LnAChR F and H that represent the most abundant subunits in the CNS (see below). Finally, responses of oocytes that co-expressed LnAChRI with LnAChRF or -J could not be distinguished from those of oocytes expressing LnAChR I alone, suggesting LnAChR I does not co-assemble into pentamers with these subunits (data not shown).

To assess the ionic selectivity of the receptors, I-V curves were determined (see "Materials and Methods") in normal or low chloride concentration. As shown in Fig. 3*E*, reduction of the chloride concentration caused no major change of the reversal potential in LnAChR A (−13 to −20 mV). In opposition, a large shift of 49 ± 1.5 mV (n = 3) was observed when the same experiment was repeated with LnAChR B receptors, which suggests that the current flowing through these receptors is mainly carried by chloride ions (Fig. 3*F*). Receptors composed of LnAChR I display comparable characteristics of chloride-selective channels (data not shown). We therefore conclude that LnAChR A contributes to cation-selective receptors, whereas LnAChR B and I contribute to anion-selective receptors.

Expression of LnAChR Subunits in the Lymnaea CNS—The distribution and level of expression of LnAChR subunits was analyzed using ISH and real time qPCR, respectively.

qPCR analysis on cDNA templates derived from various tissues and organs showed that LnAChR subunits are expressed almost exclusively in the CNS (Fig. 4). In the CNS the transcripts for the identified

A

Subunit	ACh Response (1mM)	5HT Response (1mM)	Glutamate GABA Glycine Response (1mM)
LnAChR A	+ (22)	- (4)	- (4)
LnAChR B	+ (28)	- (3)	- (3)
LnAChR C	- (7)	- (7)	- (7)
LnAChR D	- (5)	- (5)	- (5)
LnAChR E	- (6)	- (6)	- (6)
LnAChR F	- (8)	- (8)	- (8)
LnAChR F + H	- (8)	- (8)	- (8)
LnAChR F + H + C	- (8)	- (8)	- (8)
LnAChR F + H + E	- (8)	- (8)	- (8)
LnAChR F + H + J	- (8)	- (8)	- (8)
LnAChR F + H + K + J	- (8)	- (8)	- (8)
LnAChR G	- (14)	- (5)	- (5)
LnAChR H	- (8)	- (8)	- (8)
LnAChR I	+ (2)	+ (2)	- (2)
LnAChR I + F	+ (3)	+ (3)	- (3)
LnAChR I + J	+ (4)	+ (4)	- (4)
LnAChR J + C	- (6)	- (6)	- (6)
LnAChR J + D	- (8)	- (8)	- (8)
LnAChR J + E	- (8)	- (8)	- (8)
LnAChR J + F	- (8)	- (8)	- (8)
LnAChR J + H	- (8)	- (8)	- (8)
LnAChR J + K	- (8)	- (8)	- (8)
LnAChR K	- (8)	- (8)	- (8)

(n)= number of cells tested

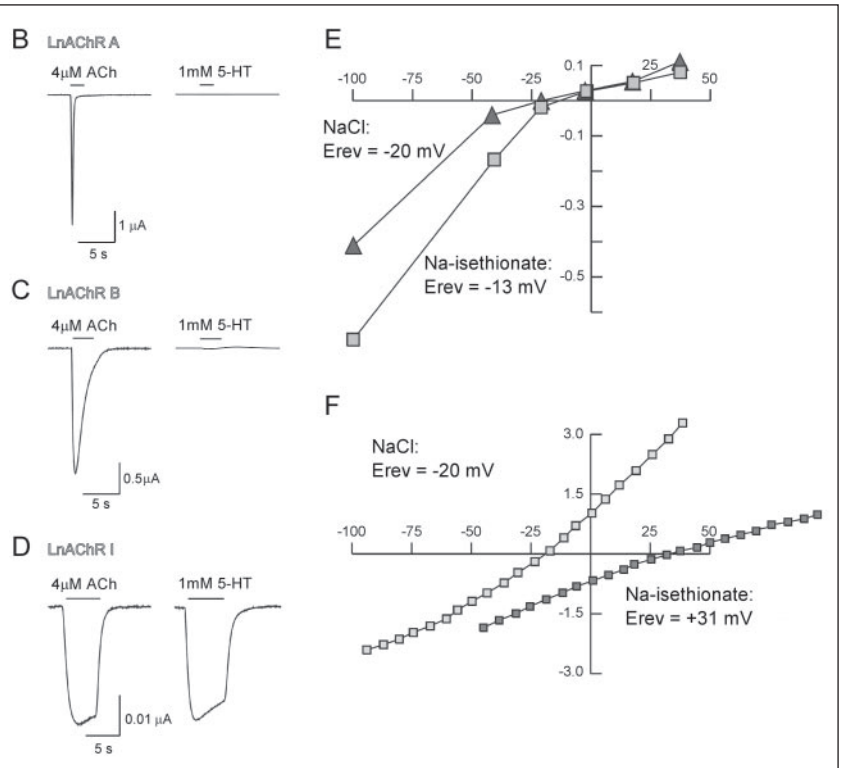

FIGURE 3. **Functional expression of LnAChR receptors in *Xenopus* oocytes.** *A,* individual LnAChR subunits or subunit combinations were expressed in *Xenopus* oocytes and assayed for currents generated by application of saturating concentrations (1 mM) of ACh, 5-HT, glutamate, GABA, and glycine. The choice of the putative subunit combinations, single, dual or triplets, was done according to the level of expression presented in Fig. 5. The + indicates functional receptors, and the − indicates the absence of agonist-evoked responses. Functional expression was observed with the LnAChR A, B, and I subunits, as well as with co-expression of the LnAChR I and F subunits. None of the combinations containing the LnAChR I subunit could be distinguished from receptors obtained with expression of LnAChR I alone. *B,* functional receptors composed of LnAChR A display a fast desensitizing current following ACh (*left*) but not 5-HT application (*right*). *C,* the LnAChR B receptor displays a similar transmitter specificity, but compared with LnAChR A it has a slower time course of desensitization. *D,* expression of the LnAChR I subunit results in a receptor that is equally responsive to application of ACh and 5-HT and shows little desensitization. Compared with LnAChR A and B, currents mediated by LnAChR I are small. Cells were held in voltage clamp at −100 mV and agonists were briefly applied during the period indicated by the *bar. E* and *F,* current-voltage relationships of receptors composed of LnAChR A or B subunits recorded under normal or low extracellular chloride concentration. To better illustrate the current-voltage relationships, line segments were drawn between data points. Values indicate the reversal potentials determined in the normal and low chloride conditions. Note the very small effect observed for the A subunit (*E*) whereas a large shift was observed for the B receptor (*F*). Each graphs reflects recordings from a single oocyte.

LnAChR subunits are exclusively found in neurons as shown by ISH (see Fig. 6). Expression was absent in non-neuronal cells in the CNS (glia and connective tissue) and in remnants of striated muscle included in the CNS tissue sections. We therefore concluded that all identified *Lymnaea* nAChR subunits are neuronal nAChR subunits.

In the CNS, LnAChR subunits are expressed at different relative expression levels (Fig. 5). LnAChR A, D, G, I, K, and L contribute to the total subunit expression in the CNS to a low degree. Most abundant are LnAChR F and H subunits that together represent approximately half of the total subunit expression. Only four subunits, LnAChR F and H together with the less abundant LnAChR C and E subunits, account for the majority of nAChR subunit expression in the CNS. Considerable differences are observed in the relative contribution of LnAChR subunits to expression at the level of individual ganglia. In most ganglia LnAChR F or H represent the most abundantly expressed subunits, in particular in the right pleural ganglion. However, some subunits display a particularly high contribution in only a few ganglia, such as LnAChR B in the buccal ganglia, LnAChR A in the left and right cerebral ganglia, and LnAChR E in the right pedal ganglion. LnAChR D and I subunits show very little contribution to expression in any of the ganglia.

The results obtained by qPCR are in good agreement with findings made using ISH (Fig. 6). Expression of LnAChR subunit transcripts can be observed in all ganglia of the *Lymnaea* CNS. The LnAChR F and H subunits are abundantly expressed throughout the CNS as indicated by numerous labeled neurons that represent ~10% of the neurons in all ganglia.

Expression of the Vesicular ACh Transporter in the Lymnaea CNS—To establish the extent of acetylcholinergic transmission in the *Lymnaea* CNS, we also mapped the expression of the ACh-synthesizing cells by identifying the cellular expression of the *Lymnaea* vesicular ACh transporter (LVAChT). The vesicular ACh transporter has been used previously as a marker of cholinergic neurons (25, 31). ISH shows strong labeling of an estimated 10% of the neurons throughout the CNS (Fig. 6). The highest relative LVAChT expression level is observed for the left pedal ganglion. LVAChT in other ganglia is lower, with the cerebral ganglia, the parietal ganglia, and the visceral ganglion representing the lowest expression (*i.e.* ≤25% of LVAChT expression in the left pedal ganglion).

Expression of LnAChR Subunits in Identified Neuronal Populations—The *Lymnaea* CNS contains various identified clusters of neurosecretory cells, which synthesize neuropeptides and have been shown to be implicated in various aspects of physiology, such as animal growth, copulation behavior, and egg laying. To investigate whether these neurons might be controlled by cholinergic transmission or whether they synthesize ACh as transmitter, the expression of LnAChR subunits and of LVAChT, respectively, was determined. Five types of neurosecretory cells were investigated, *i.e.* caudodorsal cells (CDCs, egg laying), light green cells (LGCs, growth), light yellow cells (LYCs, function unknown),

anterior lobe (AL, copulation behavior) neurons, and PeIB cluster neurons (copulation behavior).

qPCR profiling detected expression of all identified LnAChR subunits in each of these neuronal cell populations (Fig. 7). However, differences in expression levels were observed and generally were more pronounced compared with the expression detected in the complete ganglia. In view of the high sensitivity of the qPCR technique, this observation indicates that the neuronal clusters express only a selective subset of LnAChR subunits rather than the full complement. All neuronal clusters display the highest relative expression of the LnAChR F subunit, with exception of the left and right cerebral AL clusters, in which LnAChR H is most abundant.

The expression of these abundant transcripts was confirmed by *in situ* hybridization that showed a moderate labeling of LnAChR F in the CDCs and a strong labeling in the LGCs. A low level labeling is observed for other subunits, besides LnAChR F and H, such as the LnAChR I in the CDCs and LnAChR D in the LGCs. Expression of LnAChR E in the AL and PeIB neurons as indicated by qPCR was not observed with ISH. Finally, ISH reveals heterogeneity in the expression of LnAChR subunits within the neuronal populations, such as LnAChR F expressed by the lateral LGCs, but not by the medial group of LGCs. Most interestingly, CDCs display a heavy labeling when probed for LVAChT expression, suggesting the neuroendocrine CDC egg-laying hormone cells are all producing ACh, in addition to the egg-laying hormone peptides. No LVAChT labeling of the LGC, LYC, AL, and PeIB cell types was observed.

Relative LnAChR Subunit Expression Levels Determined in the Identified VD4 and LPeD1 Neurons—In principle, the newly obtained sequence information of nAChRs subunits could be used to analyze nAChR subtype expression by the identified neurons described in the *Lymnaea* CNS. As proof of principle, we determined LnAChR subunit expression in cultured LPeD1 and VD4 neurons that have been shown to express different types of functional nAChRs by means of electrophysiology (11). Although *Lymnaea* β-tubulin expression is readily detectable, expression of LnAChR subunits is close to the detection limit of the technique (C_t values 35–40). qPCR is unable to detect expression of a number of subunit types, in particular in VD4 preparations (Fig. 8). For other subunit types, *i.e.* LnAChR B, C, D, F, G, I, J, and K in LPeD1 and LnAChR C, D, F, and K in VD4, expression can be detected, but not in all preparations. Finally, expression of the LnAChR E subunit in LPeD1 could be detected in each sample. Compared with LPeD1, relative expression levels in VD4 are ~10-fold lower. The LnAChR E and F subunits that are measured most reliably in LPeD1 and VD4, respectively, display the largest mean level of expression accompanied by a large variation.

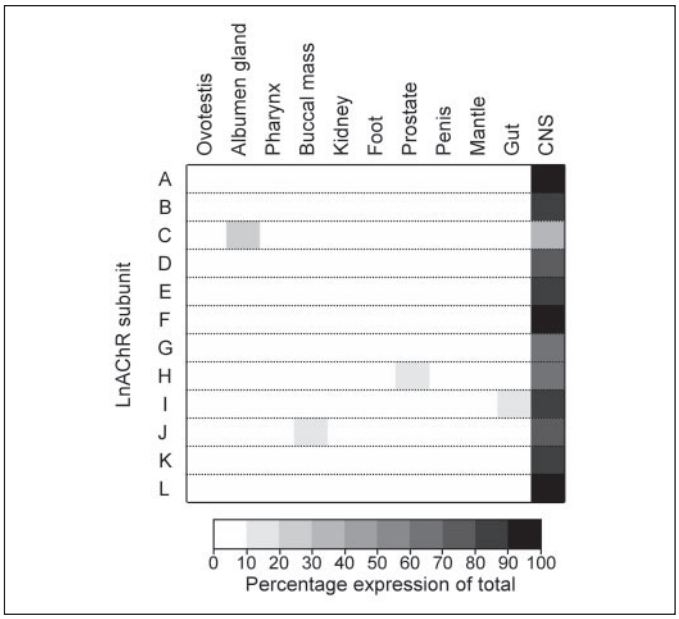

FIGURE 4. **Relative levels of expression of LnAChR subunit transcripts in *Lymnaea* organs.** Relative LnAChR subunit transcript levels were determined by real time qPCR on cDNA preparations of various *Lymnaea* organs and tissues pooled from 5 to 10 animals ($n = 1$). LnAChR transcript levels were normalized to the levels of *Lymnaea* elongation factor α. For each subunit, individual tissue measurements are expressed as a fraction of the combined expression of the subunit in all organs.

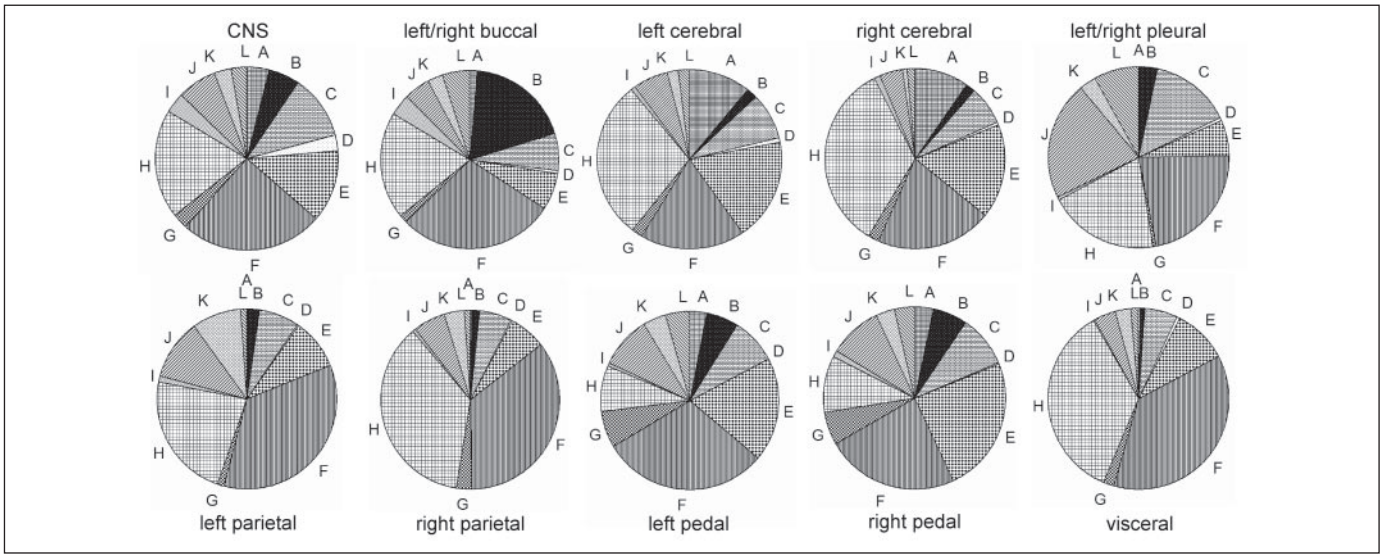

FIGURE 5. **Relative transcript expression levels of LnAChR subunits in the central ring ganglia of *L. stagnalis*.** Expression of LnAChR transcripts was measured on the cDNA preparations of independent pools of the complete CNS ($n = 17$), the left and right buccal ($n = 3$), the left cerebral ($n = 5$), the right cerebral ($n = 5$), the left and right pleural ($n = 5$), the left pedal ($n = 4$), the right pedal ($n = 3$), the left parietal ($n = 4$), the right parietal ($n = 3$), and the visceral ($n = 5$) ganglia and were normalized to the expression of *Lymnaea* β-tubulin. The *pie charts* reflect the mean expression level of LnAChR subunits relative to the total LnAChR subunit expression in the cDNA preparations. Note that data and analysis of pleural ganglia, and of buccal ganglia, are based on RNA pooled from the left and right ganglia.

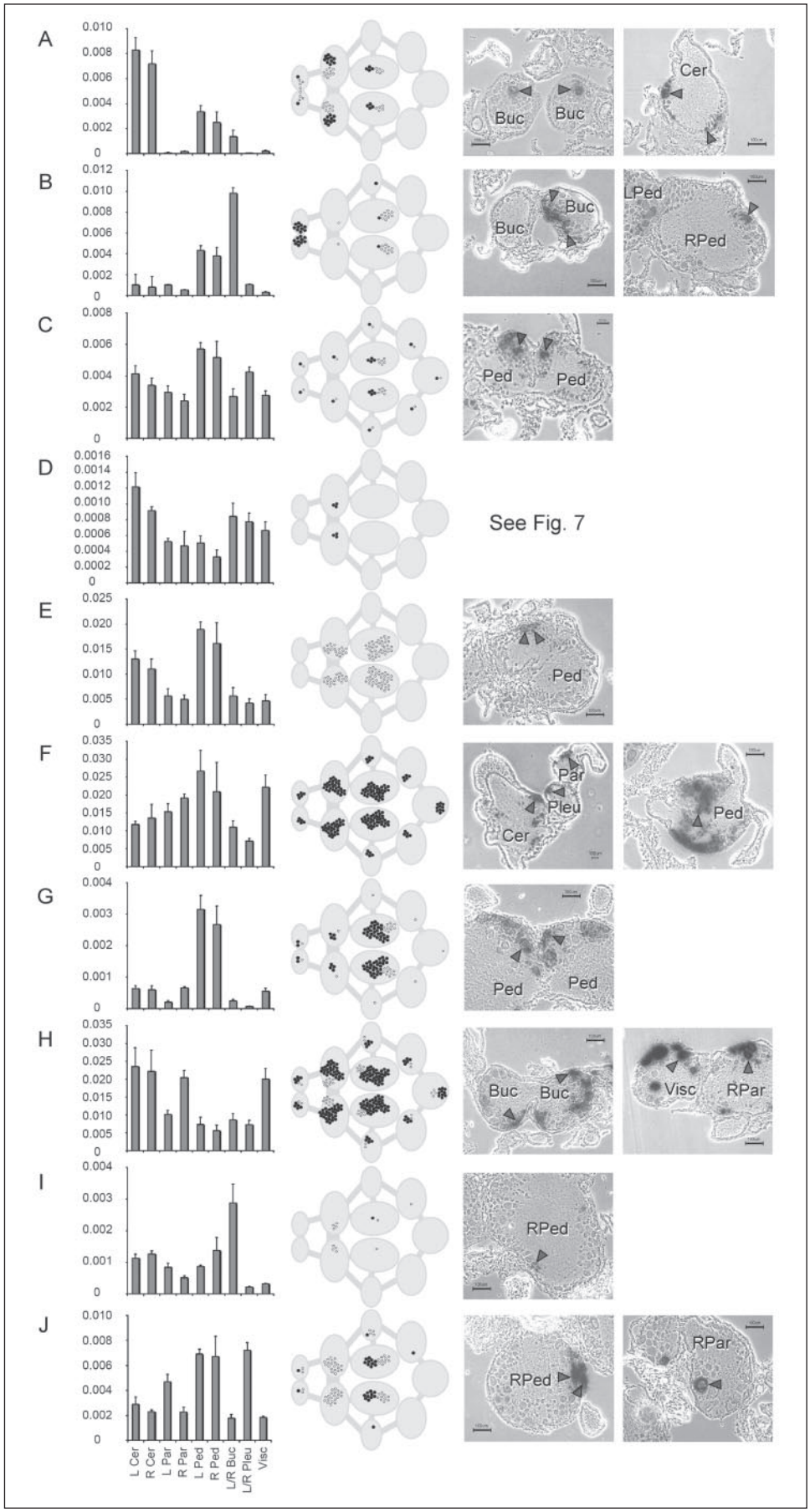

FIGURE 6. **Expression of LnAChR subunits and LVAChT in the *Lymnaea* CNS.** The expression of LnAChR subunits and of the LVAChT in the central ring ganglia of the *Lymnaea* CNS was investigated using qPCR and ISH. Each graph (*A–VAChT*) indicates the relative expression levels in the different ganglia as determined by qPCR under Fig. 5. The drawings provide an overview of the location and the intensity of labeled neurons observed with ISH; please note the number of spheres does not correspond to the exact number of neurons. The photographs show examples of labeled neurons (*black outlined arrowheads*) obtained with ISH on serial sections of the *Lymnaea* CNS. With the LVAChT, the identified RPeD1 neuron (*white outlined arrowhead*) was found unlabeled. *Scale bars* represent 100 μm. The abbreviations used are as follows: *L/R Buc*, left and right buccal ganglia; *L Cer*, left cerebral ganglion; *R Cer*, right cerebral ganglion; *L/R Pleu*, left and right pleural ganglia; *L Ped*, left pedal ganglion; *R Ped*, right pedal ganglion; *L Par*, left parietal ganglion; *R Par*, right parietal ganglion; *Visc*, visceral ganglion.

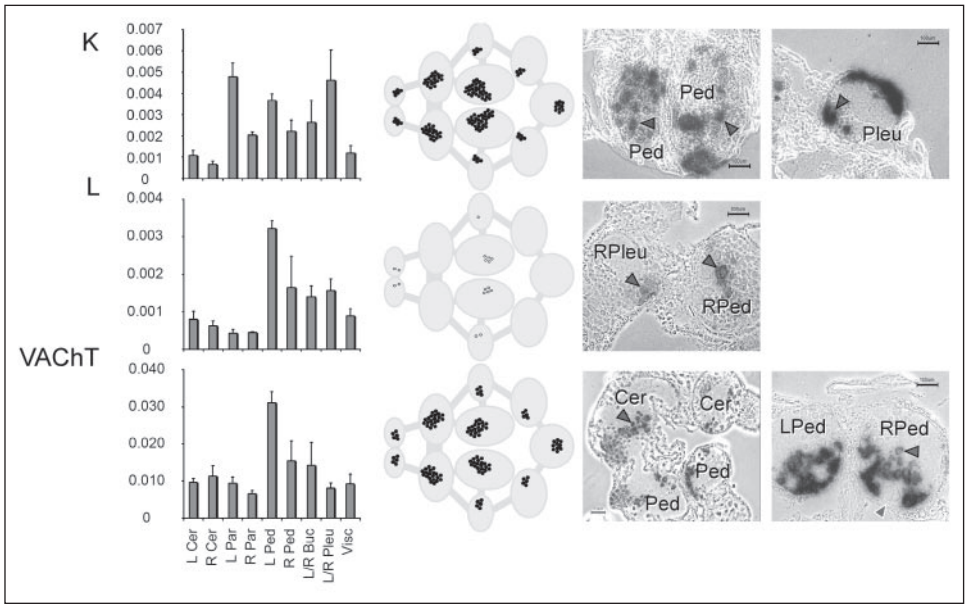

FIGURE— 6 *continued*

DISCUSSION

From the moment of the identification of ACh as a neurotransmitter, the receptors of ACh have been investigated in the CNS of molluscs by means of electrophysiology (8, 9, 12, 13, 32, 33). Molluscan CNS studies, as opposed to those in mammalian species, demonstrated that fast ACh-mediated synaptic transmission is predominant in the CNS and is mediated by multiple and unique nAChR subtypes (10, 11, 34–36). In this paper, for the first time, a comprehensive analysis of the molecular complexity of subunits potentially involved in fast cholinergic transmission in a molluscan species is presented.

LnAChR Subunit Diversity in the Lymnaea CNS—In total, we identified 10 α-type and 1 β-type full-length *Lymnaea* nAChR subunits, as well as one presumed partial nAChR subunit. Whether this describes the full complement of nAChR subunits in the *Lymnaea* CNS is unknown; however, the number of *Lymnaea* subunits characterized matches that found in other species. For instance, in the human genome 8 α-type and 3 β-type neuronal nAChR subunits exist, and insects possess 7 α-type and 2 β-type nAChR subunits, which all represent neuronal nAChR subunit types (37, 38). As in mammals and *Drosophila*, the observed nAChR subunit diversity in *Lymnaea* does not resemble the exceptionally high number of *Caenorhabditis elegans* (at least 20 α-type and 7 β-type) (39) or of the pufferfish *Fugu rubripes* (16 α-type and 12 β-type) (40).

Several observations suggest that we did not identify the full complement of LnAChR subunits. Although the partially characterized LnAChR L subunit might represent a β-type nAChR subunit (see below), we were unable to design degenerate primers that confidently target β-type subunits, which explains why the only β-type subunit was obtained from another source. Most likely, additional β-type nAChR subunits remain to be characterized. In addition, we did not observe labeling of glial cells using ISH, which suggests that the subunit(s) belonging to an α-bungarotoxin-sensitive nAChR shown in previous work to be present on AChBP-expressing glial cells (29) remain(s) to be identified.

The functional expression of the subunit types A and B reveals their sensitivity for ACh and indicates that the related subunits are also involved in the formation of nAChRs. The absence, however, of efficient functional expression of the other subunits indicates that for their functional expression additional (β) subunits are probably necessary. It is important to recall that functional expression of insect receptors was obtained only by the combination of an insect α-like subunit with a vertebrate β-type subunit (41, 42). Also, our attempts to express various α-type subunits together with the cloned and predicted β-type subunit did not result in a functional channel in *Xenopus* oocytes. Either the appropriate combination of subunits or, alternatively, accessory proteins comparable with RIC-3 (43) might be missing. Further work will be required to clarify this issue.

Evolution of Lymnaea nAChR Subunits—Sequence homology analysis shows that LnAChR A, C, E, J, and possibly L subunits are sequence-related to subunits from human and *Drosophila*. Based on this similarity, we might infer possible functional properties of these subunits. Indeed, LnAChR A that is related to the homo-oligomeric human α7 nAChR and *Drosophila* Dα6 nAChR (44, 45) also has the capability to form functional homopentameric receptors when expressed in *Xenopus* oocytes. Similarly, LnAChR J (β-type) and LnAChR C and E are related to the heteropentameric group of human nAChR subunits and can be predicted to participate in heteromeric receptors. Although insignificant with phylogenetic analysis, the partial LnAChR L subunit might be related to *Lymnaea* (LnAChR J), *Aplysia*, and *Drosophila* (ARD) β-type subunits (Fig. 2*C*), agreeing with LnAChR L most closely resembling the β-type nAChR subunits from various insects when compared with GenBank^{TM} sequences (data not shown).

Although clearly belonging to the nAChR subunits, the LnAChR B, F, I, and K and the LnAChR D and G groups display no particular similarity to individual mammalian or insect nAChR subunits. Possibly, these subunits are typical products of molluscan evolution. In line with this, LnAChR B and LnAChR I, and most likely LnAChR F and K, seem to represent constituents of the long known chloride-conducting nAChR subtypes known so far to only exist in molluscs (9, 12–15). The results of BLAST analysis and the presence of specific residues in loop C of ligand binding conserved in α-type nAChR subunits to a large extent support classification of LnAChR H as an α-type nAChR subunit. Phylogenetic analysis, however, suggests that LnAChR H has diverged considerably from nAChR subunits appearing almost as distant from human nAChR subunits as from 5-HT$_3$ receptor subunits. In addition, the histidine residue in loop C of ligand binding of LnAChR H is difficult to reconcile with an interaction with the quaternary ammonium of ACh, an interaction suggested for tyrosines at corresponding positions conserved in

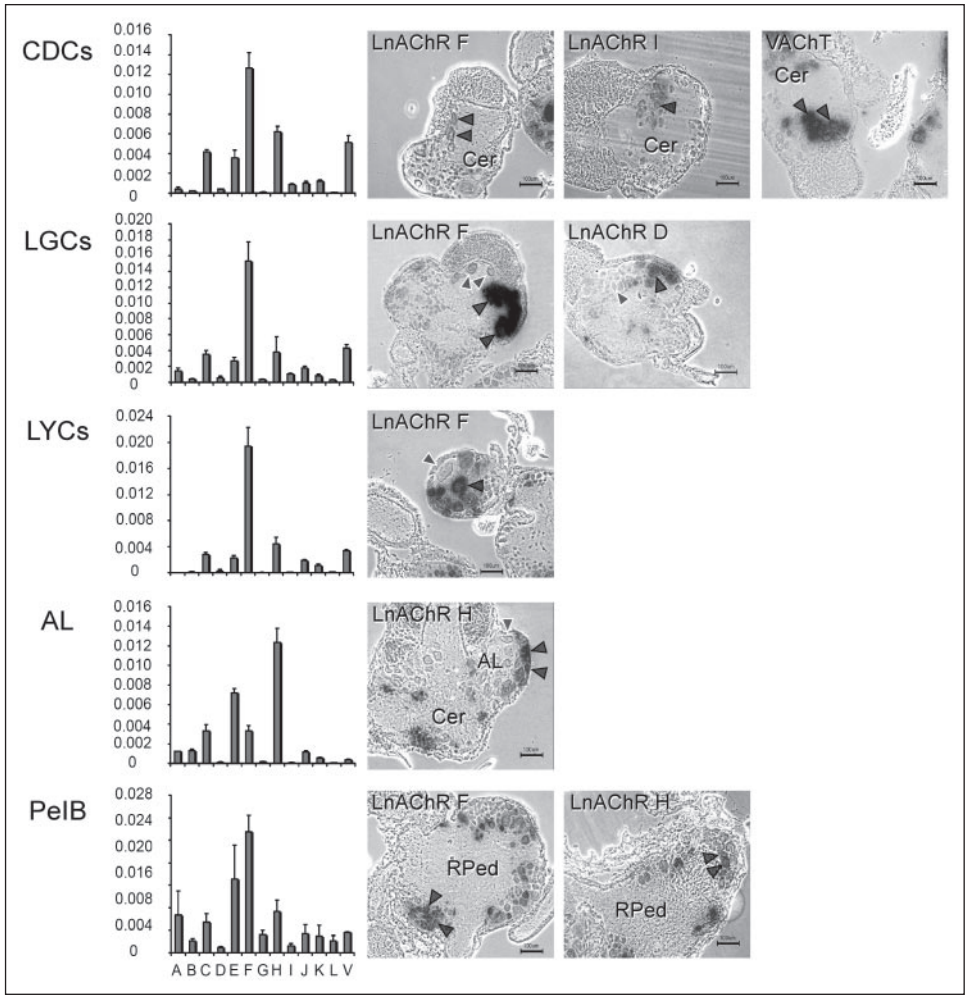

FIGURE 7. **Expression of LnAChR subunits in identified neuronal populations in the *Lymnaea* CNS.** The expression of the LnAChR subunits and of the LVAChT by the CDCs, the LGCs, the LYCs, and neurons of the AL, and PeIB cluster (*PeIB*) was investigated using qPCR and ISH. The *graphs* represent relative expression levels of LnAChR subunits (*A–L*) as well as of LVAChT (*V*) as determined by qPCR on cDNA preparations ($n = 3$) of freshly dissected neurons. The *photographs* show examples of observed ISH labeling of neuronal populations identified in serial sections of the *Lymnaea* CNS. *Scale bars* represent 100 μm.

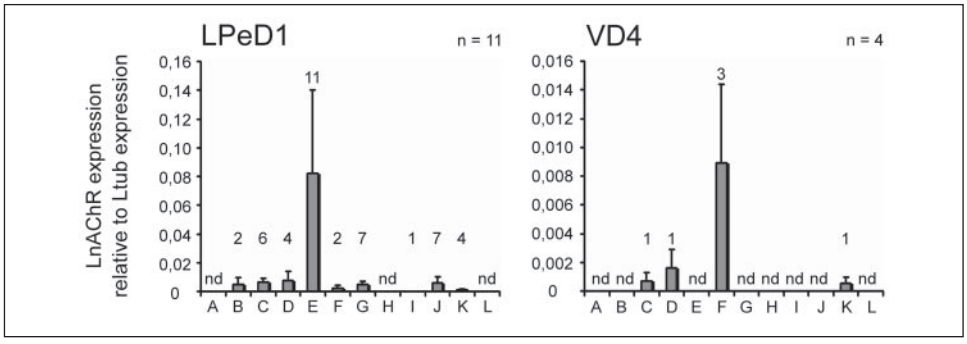

FIGURE 8. **Relative expression levels of LnAChR subunits in cultured LPeD1 and VD4 neurons.** Expression levels of LnAChR subunits were determined by qPCR on cDNA preparations of independent pools of LPeD1 or VD4 neurons. Expression levels are expressed as the mean ratio of LnAChR subunit expression *versus Lymnaea* β-tubulin (*Ltub*) expression $\pm$ S.E. *Numbers* on *top* of *bars* indicate the number cDNA preparations that gave detectable levels of the corresponding transcript. Samples without any detectable subunit expression were excluded. *nd*, not detectable.

other α-type nAChR subunits (46). In conclusion, the contribution of LnAChR H to ligand binding of LGICs remains to be determined and might involve sensitivity to neurotransmitters other than ACh. The widespread presence of LnAChR H in the *Lymnaea* CNS suggests that this particular subunit mediates a general physiological function, which also pledges further functional characterization.

Acetylcholine-mediated Transmission in the Lymnaea CNS—The data presented in this paper for the first time provide a CNS-wide description of the expression of molecular components involved in cellular reception and vesicular release of acetylcholine in *L. stagnalis*. Based on our study, nAChRs are detectably expressed by at least 10% of the neurons in the CNS. That this number might actually be higher comes from reports that suggest that virtually all neurons in the *Lymnaea* CNS respond to application of ACh through presumed nicotinic receptors that are mainly depolarizing and excitatory in nature (8, 9). Our data reveal large differences in expression levels and distribution patterns of LnAChR subunit types and suggest the presence of nAChR subtypes with ganglion specificity (LnAChR A or B), cell type specificity (LnAChR D), and of subunits involved in more generic tasks (LnAChR F and H).

The expression of LVAChT reveals large numbers of acetylcholine-synthesizing neurons present in all ganglia of the *Lymnaea* CNS. Although cholinergic interneurons have been identified, the molluscan CNS is known to contain numerous motor neurons possibly accounting for many of the cholinergic neurons. For example, Giller and Schwartz (47) have functionally identified most cholinergic neurons in the *Aply-*

sia abdominal ganglion, corresponding to the visceral and parietal ganglia of *Lymnaea*, as being visceral motor neurons targeting muscle cells.

The expression of LnAChR subunits by identified neuroendocrine cell populations suggests that the release of peptides produced by these cells is under cholinergic control. Most interestingly, the heterogeneous LnAChR subunit expression pattern within the LGC (48), LYC (49), and AL (50) neuronal populations corresponds to the functional diversity observed for the expression of neuropeptides within these neuronal clusters. For instance, the different levels of transcripts for insulin-related peptides in the lateral and medial LGCs correlate with the differential expression of the nAChR F subunits in these cells. Together, these observations suggest a fine-tuned cholinergic modulation of neuropeptide release. Of all identified neuronal cell groups examined, the egg-laying hormone producing CDCs were described previously to express nAChRs involved in the regulation of neuropeptide release (51, 52). CDCs extend neurites into the cerebral commissure, which serves as the neurohemal area for the egg-laying hormone and other neuropeptides from the same precursor protein. Because the CDCs have no postsynaptic partners, the cholinergic phenotype of CDCs might point at ACh-mediated autoregulation analogous to autoregulation by neuropeptides of CDC neurons (53).

The LPeD1 and VD4 neurons in culture have been shown to express excitatory and inhibitory nAChR subtypes, respectively (54). Although qPCR fails to measure accurately the low level of LnAChR subunit expression in these neurons, the reliability of recurrent detection of certain transcripts might indicate participation of certain subunits in functionally expressed nAChRs. In particular, LnAChR E in LPeD1 and LnAChR F in VD4 are attractive candidates for additional functional analysis, for instance RNA interference-mediated knockdown of subunit expression (55). Participation of LnAChR E and F in excitatory and inhibitory nAChR subtypes, respectively, in LPeD1 and VD4 would agree with a presumed participation of LnAChR F in anion-selective receptor channels (see above).

The data described in this study, together with reports of cholinergic transmission in identified neuronal networks in molluscs, suggest a widespread use of cholinergic transmission by the molluscan CNS, which involves a number of nAChR subtypes that are comparable with mammals. However, as it appears, the *Lymnaea* nAChR subunits can be divided into definite subgroups, of which members must contribute to anionic *versus* cationic channels. As such, the *Lymnaea* subunits might contribute to a more substantial and functional complexity of the receptors generated than is observed for mammals.

Acknowledgment—We thank Leonid L. Moroz (The Whitney Laboratory, University of Florida) for the kind gift of Lymnaea nAChR subunit ESTs.

REFERENCES

1. Corringer, P. J., Le Novere, N., and Changeux, J. P. (2000) *Annu. Rev. Pharmacol. Toxicol.* **40,** 431–458
2. Alkondon, M., Pereira, E. F., and Albuquerque, E. X. (1998) *Brain Res.* **810,** 257–263
3. Grady, S. R., Meinerz, N. M., Cao, J., Reynolds, A. M., Picciotto, M. R., Changeux, J. P., McIntosh, J. M., Marks, M. J., and Collins, A. C. (2001) *J. Neurochem.* **76,** 258–268
4. Clarke, P. B., and Reuben, M. (1996) *Br. J. Pharmacol.* **117,** 595–606
5. Kaiser, S., and Wonnacott, S. (2000) *Mol. Pharmacol.* **58,** 312–318
6. Reuben, M., and Clarke, P. B. (2000) *Neuropharmacology* **39,** 290–299
7. Wonnacott, S., Kaiser, S., Mogg, A., Soliakov, L., and Jones, I. W. (2000) *Eur. J. Pharmacol.* **393,** 51–58
8. Zeimal, E. V., and Vulfius, C. A. (1967) in *Neurobiology of Invertebrates* (Salanki, J., ed) pp. 255–265, Academiai Kiado, Budapest, Hungary
9. Vulfius, E. A., Veprintzev, B. N., Zeimal, E. V., and Michelson, M. J. (1967) *Nature* **216,** 400–401
10. Yeoman, M. S., Parish, D. C., and Benjamin, P. R. (1993) *J. Neurophysiol.* **70,** 37–50
11. Woodin, M. A., Munno, D. W., and Syed, N. I. (2002) *J. Neurosci.* **22,** 505–514
12. Chiarandini, D. J., and Gerschenfeld, H. M. (1967) *Science* **156,** 1595–1596
13. Chiarandini, D. J., Stefani, E., and Gerschenfeld, H. M. (1967) *Science* **156,** 1597–1599
14. Chemeris, N. K., Kazachenko, V. N., Kislov, A. N., and Kurchikov, A. L. (1982) *J. Physiol.* (*Lond.*) **323,** 1–19
15. Vulfius, C. A., Tumina, O. B., Kasheverov, I. E., Utkin, Y. N., and Tsetlin, V. I. (2005) *Neurosci. Lett.* **373,** 232–236
16. Hamakawa, T., Woodin, M. A., Bjorgum, M. C., Painter, S. D., Takasaki, M., Lukowiak, K., Nagle, G. T., and Syed, N. I. (1999) *J. Neurosci.* **19,** 9306–9312
17. van der Steen, W. J., van der Hoven, N. P., and Jager, J. C. (1969) *Neth. J. Zool.* **19,** 131–139
18. Schultz, J., Copley, R. R., Doerks, T., Ponting, C. P., and Bork, P. (2000) *Nucleic Acids Res.* **28,** 231–234
19. Thompson, J. D., Gibson, T. J., Plewniak, F., Jeanmougin, F., and Higgins, D. G. (1997) *Nucleic Acids Res.* **25,** 4876–4882
20. Sigrist, C. J., Cerutti, L., Hulo, N., Gattiker, A., Falquet, L., Pagni, M., Bairoch, A., and Bucher, P. (2002) *Brief. Bioinform.* **3,** 265–274
21. Gattiker, A., Gasteiger, E., and Bairoch, A. (2002) *Appl. Bioinformatics* **1,** 107–108
22. Blom, N., Gammeltoft, S., and Brunak, S. (1999) *J. Mol. Biol.* **294,** 1351–1362
23. Bertrand, D., Ballivet, M., and Rungger, D. (1990) *Proc. Natl. Acad. Sci. U. S. A.* **87,** 1993–1997
24. van Minnen, J., and van Kesteren, R. (1999) in *Modern Techniques in Neuroscience Research* (Windhorst, U., and Johansson, H., eds) pp. 57–88, Springer-Verlag, Heidelberg
25. Spafford, J. D., Munno, D. W., van Nierop, P., Feng, Z. P., Jarvis, S. E., Gallin, W. J., Smit, A. B., Zamponi, G. W., and Syed, N. I. (2003) *J. Biol. Chem.* **278,** 4258–4267
26. Koert, C. E., Spencer, G. E., van Minnen, J., Li, K. W., Geraerts, W. P., Syed, N. I., Smit, A. B., and van Kesteren, R. E. (2001) *J. Neurosci.* **21,** 5597–5606
27. Harvey, R. J., Vreugdenhil, E., Zaman, S. H., Bhandal, N. S., Usherwood, P. N., Barnard, E. A., and Darlison, M. G. (1991) *EMBO J.* **10,** 3239–3245
28. Hutton, M. L., Harvey, R. J., Earley, F. G., Barnard, E. A., and Darlison, M. G. (1993) *FEBS Lett.* **326,** 112–116
29. Smit, A. B., Syed, N. I., Schaap, D., van Minnen, J., Klumperman, J., Kits, K. S., Lodder, H., van der Schors, R. C., van Elk, R., Sorgedrager, B., Brejc, K., Sixma, T. K., and Geraerts, W. P. (2001) *Nature* **411,** 261–268
30. Brejc, K., van Dijk, W. J., Klaassen, R. V., Schuurmans, M., van der Oost, J., Smit, A. B., and Sixma, T. K. (2001) *Nature* **411,** 269–276
31. Arvidsson, U., Riedl, M., Elde, R., and Meister, B. (1997) *J. Comp. Neurol.* **378,** 454–467
32. Tauc, L., and Gerschenfeld, H. M. (1961) *Nature* **192,** 366–367
33. Tauc, L., and Gerschenfeld, H. M. (1962) *J. Neurophysiol.* **25,** 236–262
34. Blankenship, J. E., Wachtel, H., and Kandel, E. R. (1971) *J. Neurophysiol.* **34,** 76–92
35. Kandel, E. R., Frazier, W. T., and Wachtel, H. (1969) *J. Neurophysiol.* **32,** 496–508
36. Wachtel, H., and Kandel, E. R. (1967) *Science* **158,** 1206–1208
37. Jones, A. K., Grauso, M., and Sattelle, D. B. (2005) *Genomics* **85,** 176–187
38. Sattelle, D. B., Jones, A. K., Sattelle, B. M., Matsuda, K., Reenan, R., and Biggin, P. C. (2005) *BioEssays* **27,** 366–376
39. Jones, A. K., and Sattelle, D. B. (2004) *BioEssays* **26,** 39–49
40. Jones, A. K., Elgar, G., and Sattelle, D. B. (2003) *Genomics* **82,** 441–451
41. Bertrand, D., Ballivet, M., Gomez, M., Bertrand, S., Phannavong, B., and Gundelfinger, E. D. (1994) *Eur. J. Neurosci.* **6,** 869–875
42. Schulz, R., Sawruk, E., Mulhardt, C., Bertrand, S., Baumann, A., Phannavong, B., Betz, H., Bertrand, D., Gundelfinger, E. D., and Schmitt, B. (1998) *J. Neurochem.* **71,** 853–862
43. Williams, M. E., Burton, B., Urrutia, A., Shcherbatko, A., Chavez-Noriega, L. E., Cohen, C. J., and Aiyar, J. (2005) *J. Biol. Chem.* **280,** 1257–1263
44. Lansdell, S. J., and Millar, N. S. (2004) *J. Neurochem.* **90,** 479–489
45. Peng, X., Katz, M., Gerzanich, V., Anand, R., and Lindstrom, J. (1994) *Mol. Pharmacol.* **45,** 546–554
46. Celie, P. H., van Rossum-Fikkert, S. E., van Dijk, W. J., Brejc, K., Smit, A. B., and Sixma, T. K. (2004) *Neuron* **41,** 907–914
47. Giller, E., Jr., and Schwartz, J. H. (1968) *Science* **161,** 908–911
48. Meester, I., Ramkema, M. D., van Minnen, J., and Boer, H. H. (1992) *Cell Tissue Res.* **269,** 183–188
49. Smit, A. B., Hoek, R. M., and Geraerts, W. P. (1993) *Cell. Mol. Neurobiol.* **13,** 263–270
50. De Lange, R. P., van Golen, F. A., and van Minnen, J. (1997) *Neuroscience* **78,** 289–299
51. Ter Maat, A., and Lodder, J. C. (1980) *Comp. Biochem. Physiol. C* **66,** 115–119
52. Ter Maat, A., Roubos, E. W., Lodder, J. C., and Buma, P. (1983) *J. Neurophysiol.* **49,** 1392–1409
53. Brussaard, A. B., Schluter, N. C., Ebberink, R. H., Kits, K. S., and Ter Maat, A. (1990) *Neuroscience* **39,** 479–491
54. Meems, R., Munno, D., van Minnen, J., and Syed, N. I. (2003) *J. Neurophysiol.* **89,** 2611–2619
55. van Diepen, M. T., Spencer, G. E., van Minnen, J., Gouwenberg, Y., Bouwman, J., Smit, A. B., and van Kesteren, R. E. (2005) *Mol. Cell. Neurosci.* **29,** 74–81
56. Le Novere, N., and Changeux, J. P. (2001) *Nucleic Acids Res.* **29,** 294–295
57. van Nierop, P., Keramidas, A., Bertrand, S., van Minnen, J., Gouwenberg, Y., Bertrand, D., and Smit, A. B. (2005) *J. Neurosci.* **25,** 10617–10626